Comparison of Summer and Winter California Central Valley Aerosol Distributions from Lidar and MODIS Measurements

Jasper Lewis[1], Russell De Young[2], D. Allen Chu[3]

[1]Center for Atmospheric Science, Hampton University, Hampton, VA 23681
[2]Science Directorate, NASA Langley Research Center, Hampton, VA 23681
[3]Goddard Earth Science and Technology Center, University of Maryland Baltimore County, Greenbelt, MD 20771

Abstract

Aerosol distributions from two aircraft lidar campaigns conducted in the California Central Valley are compared in order to identify seasonal variations. Aircraft lidar flights were conducted in June 2003 and February 2008. While the $PM_{2.5}$ concentration is highest in the winter, the aerosol optical depth measured from MODIS is highest in the summer. A seasonal comparison shows that $PM_{2.5}$ in the winter can exceed summer PM2.5 by 55%, while summer AOD exceeds winter AOD by 43%. Higher temperatures wildfires in the summer produce elevated aerosol layers that are detected by satellite measurements, but not surface particulate matter monitors. Measurements of the boundary layer height from lidar instruments are necessary to incorporate satellite measurements with air quality measurements.

1. Introduction

The California Central Valley is a major agricultural area stretching some 600 km from north to south and is one of the most productive agricultural regions in the world. The southern half of the valley is known as the San Joaquin Valley encompassing nearly 65,000 km^2, lying 300 m below sea level. The valley has cool wet winters and hot dry summers. On the western edge of the valley is the Coast Mountain range with peaks reaching 1,530 m. On the east side is the Sierra Nevada range (max 4,418 m) and the

Tehachapi Mountains (max 2,432 m) form the southern boundary of the Valley, which contain mountain passes to the Los Angeles basin and the Mojave Desert. The surrounding mountains prevent ventilation of air masses, causing pollutants and their precursors to be retained in the valley. The valley topography and climate create ideal conditions for trapping and holding pollutants within the valley. The particle and gaseous emissions can recirculate within the valley and accumulate to unhealthy levels.

The valley is currently a nonattainment area with the $PM_{2.5}$ National Ambient Air Quality Standard (NAAQS) because measurements of several monitoring sites exceed the annual $PM_{2.5}$ standard, especially in the lower part of the valley (Geis, 2007) where air quality is a significant health issue. Significant progress has been made in reducing the PM_{10} and $PM_{2.5}$ emissions and a plan is in place to meet the NAAQS and state standards for air quality (SJV Air Pollution Control District, 2008a).

It should be noted however that valley emissions are not dominated by a single source. The observed $PM_{2.5}$ levels represent aggregated urban emissions with contributions from the region. The local climate produces seasonal variations in particulate levels through the changes in atmospheric conditions that affect the types of emissions, emission rates, and atmospheric formation of particles from precursor emissions.

During fall and winter, meteorological conditions contribute to low wind speeds, low-lying inversion layers and increased secondary particle formation, all establishing a situation conducive to the formation and accumulation of $PM_{2.5}$. Colder, frequently stagnant conditions occurring in December and January favor formation of ammonium nitrate, and thus experience the highest levels of ground $PM_{2.5}$. The cold weather also

induces the public to increase residential wood burning that further adds emissions to the atmosphere. During the winter, wind direction varies from the south-southeasterly directions to north-northwesterly directions. Temperature inversion traps $PM_{2.5}$ below the mixing height, remaining more concentrated than when it is allowed to mix more freely with cleaner air at higher altitudes. This contributes to higher $PM_{2.5}$ concentrations as inversions are formed more persistently (stable) during the winter months, when inversions occur from 15 to 300 meters.

In the summer, long periods of little or trace rainfall result in extreme dryness of soils along roadways, increasing emissions from traffic movement. Limited rainfall during the summer months reduce the frequency of events that clear emissions from the local area. At night, cooler drainage winds from the surrounding mountains prevent exit of the air at the southern end of the Valley, causing recirculation of pollutants in a counterclockwise pattern and returning polluted air to urban areas. Throughout the valley, some of the pollutants transported to higher altitudes from daytime heating return to the surface at night by drainage winds from the mountains. In the spring and summer $PM_{2.5}$ tends to be lower with mostly motor vehicle emissions, secondary sulfate, and primary geological material from the fine particle fraction of airborne soil. Daytime temperature inversions during the summer are usually not encountered until 610 to 760 meters above the surface (SJV Air Pollution Control District, 2008b).

Figure 1 summarizes the seasonal trends and chemical components of $PM_{2.5}$ near Bakersfield, California in the lower valley. Winter and spring months are heavily dominated by secondary ammonium nitrate with moderate contributions of secondary sulfate, motor vehicle emissions, primary geological material and direct emission of

organic aerosols identified as biomass burning from wood combustion, wild fires or agricultural burning. In the summer, organic carbon and ammonium sulfate dominate the composition of $PM_{2.5}$.

The primary transport route into the Valley is through the northwest in the vicinity of Stockton where transport is directed from Stockton to Bakersfield for all the months except January and February. During the summer the air into the valley is directed from the northwest at all hours of the day. The primary transport route out of the valley is over the Tehachapi Mountains at the southeast of Bakersfield. This outflow pattern contributes significantly to the pollution in the Mojave Desert. The flow over the Tehachapi Mountains is most effective during the summer and nearly absent during winter periods because of stagnation. Upslope flow occurring during the afternoon throughout the year is effective in removing pollutants from foothills of the valley. A portion of the pollutants; however, is returned to the valley by the nocturnal drainage winds. Ventilation of the valley during the summer leads to a typical pollution residence time of 1-2 days, dependent upon location. During the winter, because of stagnation, typical residence times of 2-8 days may be experienced. In general, the air at ground level is warmed by sunlight causing it to rise and carry emissions aloft. This rising air pattern mixes the fresh emissions with air at higher elevations, dispersing the emissions and reducing the concentration of directly emitted $PM_{2.5}$ and precursors. However, temperature inversion layers frequently block the rising air recirculating it down to the surface. (Smith et al., 1981).

Aircraft lidar flights are rare in the valley. The first occurred in September 1994, that flew a 1064-nm lidar over the lower valley near Bakersfield as validation for the

Lidar In-Space Technology Experiment (LITE) (Strawbridge and Hoff, 1996). This paper will compare more recent results from two airborne aerosol lidar campaigns over the San Joaquin Valley. The first campaign occurred in June 2003 (De Young et al., 2005) and the second in February 2007 (Al-Saadi et al., 2008). These two lidar campaigns provide contrasted aerosol conditions in summer and winter. The lidar returns will be used to derive aerosol optical density (AOD) and compared with the MODIS (Moderate Resolution Imaging Spectroradiometer) AOD from the Terra and Aqua satellites. The advantage of aerosol lidar is that it provides the high-resolution vertical distribution of aerosols. Though it does not give the number density of aerosols, it does measure the boundary layer height accurately, which is important since most of the $PM_{2.5}$ aerosols are confined within boundary layer. Lidar can also be used to determine the height of aerosol plumes above the boundary layer, which can be transported from great distances. Lidar with multiple wavelengths and depolarization can be used to classify aerosol types (Sasano and Browell, 1989). While lidar gives high vertical but low spatial resolution, satellite AOD measurements give a very broad coverage but columnar measurement at moderate resolutions. The synthesized lidar and satellite measurements can result in a better understanding of aerosols with ground $PM_{2.5}$ concentrations for health and regulatory needs over a large area. This paper will examine lidar and MODIS AOD measurements in correlating ground $PM_{2.5}$ concentrations with back trajectories in aid of tracking origins of air mass to give a clearer picture of the distribution of aerosols within the valley.

2. Experimental Configuration

Two different aircraft lidar systems were used in this study. The 2003 lidar measurements were made using the Compact Aerosol Lidar (CAL) deployed on the NASA DC-8 during the DC-8 Inlet/Instrument Characterization Experiment (DICE), while the 2007 lidar measurements were made using the Airborne High Spectral Resolution Lidar (HSRL) deployed on the NASA King Air B-200. A summary of the two lidar systems is shown in Table 1.

2.1 Compact Aerosol Lidar (CAL)

The CAL used in the 2003 San Joaquin Valley campaign was built in the Science Directorate of NASA Langley Research Center (DeYoung et al., 2005; Gili and DeYoung, 2006). The standard backscatter lidar system, depicted in Figure 2, has dimensions of 108-cm x 64-cm x 53-cm and a mass of 115-kg and was flown on the NASA DC-8. The laser is a frequency doubled Nd:YAG (Big Sky Laser - Quantel) with a 20-Hz repetition rate. The 1064-nm and 532-nm energies are typically 60-mJ and 80-mJ, respectively. A steerable 45^{o} turning mirror is used to align the transmitted beam to the telescope. The atmospheric return passes to the receiver box by a 1-mm diameter optical fiber coupled to the focal point of a 0.30-m diameter telescope.

The received light is collimated and split into 1064-nm and 532-nm channels, with a further split of the 532-nm wavelength into analog (90%) and photon counting (10%) channels. The 1064-nm return passes through a 1-nm full-width-at-half-maximum (FWHM) filter before being focused onto an avalanche photodiode (APD) detector. The 532-nm return passes through a 0.5-nm FWHM filter before being split between analog and photon-counting photomultiplier detectors. Data is averaged over a 2-s (40 shots) time interval before being stored by the computer.

2.2 Airborne High Spectral Resolution Lidar (HSRL)

The Airborne HSRL used in the 2007 San Joaquin Valley campaign was also developed in the Science Directorate of NASA Langley Research Center (Hair et al., 2008) and deployed on the NASA King Air B-200. The HSRL takes advantage of Doppler broadening to independently resolve the molecular and aerosol atmospheric lidar returns. Backscattered radiation from air molecules is Doppler broadened on the order of GHz due to the high-velocity random thermal motion of the molecules. By contrast, slower-velocity aerosol particles are only Doppler broadened on the order of MHz due to their much larger mass. An extremely narrow-band iodine vapor (I_2) absorption filter is used to separate the molecular return from the aerosol return at the 532-nm wavelength. The HSRL instrument also functions as a standard backscatter lidar at the 1064-nm wavelength.

The HSRL system depicted in Figure 2, uses a 200-Hz pulsed Nd:YAG laser (Fibertek). The 1064-nm and 532-nm energies are 1.1-mJ and 2.5-mJ, respectively. The receiver employs a 40-cm telescope with a 1-mrad field of view. The transmitter and receiver occupy a volume with dimensions of 83-cm x 56-cm x 76-cm, while the data acquisition and control system occupies an additional 0.37-m^3.

The 1064-nm lidar return passes through a 0.4-nm FWHM interference filter before being separated into parallel and perpendicular polarization channels, which distinguishes between spherical and nonspherical particles. The 532-nm lidar return passes through a temperature tuned, 60-pm etalon, (Coronado), and then splits between the boresight detector (4%) which maintains alignment between the transmitter and receiver, the parallel and perpendicular polarization channels (10%), and the I_2 filter and

molecular return channel (86%). Data is typically averaged over a 0.5-s (100 shots) time interval before being stored by the computer.

2.3 Moderate Resolution Imaging Spectroradiometer (MODIS)

MODIS is a 36-channel spectroradiometer onboard both Terra and Aqua satellites of the Earth Observing Systems (EOS). The MODIS spectral channels used in retrieving aerosol optical depth (AOD) over land and ocean include two 250-m (660 and 860-nm channels), and five 500-m (470, 550, 1240, 1640, and 2130-nm) channels. The 250-m resolution 660 nm and 860 nm channels are used to detect water bodies such as lakes or rivers. Then the aggregated 500-m resolution 660-nm and 860-nm reflectances together with other 500-m channels are used to derive aerosol optical depths. The detailed methodology of the MODIS aerosol algorithm for the procedures of screening clouds and surface snow/ice was described by Remer et al. (2006). At the final step, pixels that pass screenings are further analyzed for AOD retrieval. For example, in a 10 km grid, pixels are further selected by a 20-50 percentile by removing the upper 50% and the lower 20% of the pixels to avoid possible sub-pixel contamination by clouds, surface snow/ice, and water bodies. The algorithm requires the final number of pixels to be greater than 12 to have a valid retrieval. Otherwise, the algorithm reports a missing AOD retrieval. Over vegetated and semi-arid surfaces where AOD values are shown as the majority of MODIS retrievals, the AOD products have been widely used in routine air quality monitoring, such as Infusing satellite Data into Environmental Applications (IDEA) (http://idea.umbc.edu) (Al-Saddi et al, 2007) and in correlating with surface $PM_{2.5}$ concentrations for public health related studies (Kumar et al., 2007; Kumar et al., 2008)

MODIS 5x5-km AOD products are derived based upon the operational 10x10-km algorithm with 100 available pixels. Thus the degree of freedom in selecting the best pixels is largely reduced. To maintain the quality of retrieval as the operational 10x10-km retrievals, we choose to use the same requirement of minimum number of pixels – 12 pixels for the 5x5-km retrievals. Though the number of available pixels is significantly reduced (by a factor of 4 from 10 km to 5 km), the quality of the retrieval, however, is retained, which is important for the case studies with variable clouds above the California Central Valley. Note that the 5x5-km AOD retrievals are derived only over land for comparisons with 10x10-km AOD values in correlating with $PM_{2.5}$ ground measurements.

3. Results

The data used for comparison between the summer and winter San Joaquin Valley campaigns were collected on the dates of June 3, 5, 11, 12, and 17 of 2003 using the CAL, and the dates of February 15, 16, and 17 of 2007 using the Airborne HSRL. For each campaign, comparisons of the lidar derived AOD (532-nm) to MODIS AOD (550-nm), AERONET AOD (500-nm), wind back trajectories, $PM_{2.5}$ and PM_{10} mass concentrations, and lidar extinction profiles (1064-nm) will be presented.

While the winter 2007 lidar flights were conducted to fly over $PM_{2.5}$ stations stretched from the northern end to the southern end of the San Joaquin Valley, the summer 2003 lidar flights were mainly focused on the southern part of the valley. Since both campaigns conducted flights over Bakersfield, special attention will be given to the Bakersfield area data.

3.1 Summer 2003 Campaign

The 532-nm wavelength was unavailable during this campaign; therefore, the lidar derived AOD was obtained by converting the 1064-nm AOD to a 532-nm AOD using the Angstrom exponent. The power returned to the lidar receiver, *P*(z), is given by the lidar equation as:

$$P(z) = \frac{C}{z^2}[\beta_m(z) + \beta_a(z)]T^2(z). \quad (1)$$

C is the calibration constant, $\beta_m(z)$ is the molecular backscattering coefficient, $\beta_a(z)$ is the aerosol backscattering coefficient, and *T*(*z*) is the one-way transmittance from the lidar to the height *z*. The lidar data is inverted using the Fernald method (Fernald et al., 1972; Fernald, 1984) to determine the aerosol backscatter coefficient, β_a. The lidar AOD, τ, is calculated as:

$$\tau = S_a \int_0^{Z^*} \beta_a(z)dz \quad (2)$$

where S_a is the lidar ratio and Z^* is an altitude where it is assumed only molecular scattering occurs ($\beta_a(Z^*) = 0$).

For two different wavelengths λ_{1064} and λ_{532} the Angstrom exponent, γ, relates the optical thicknesses τ_{1064} and τ_{532} such that:

$$\tau_{532} = \tau_{1064}\left(\frac{\lambda_{532}}{\lambda_{1064}}\right)^{-\gamma}. \quad (3)$$

In this calculation, it was assumed that the Angstrom exponent for the 500-nm and 1020-nm AERONET wavelengths measured from Fresno, CA could be used for the 532-nm and 1064-nm lidar wavelengths with negligible error. Optical depths calculated using Equation 3 are referred to as the converted 532-nm AOD in the sections that follow. The

1064-nm lidar ratio was selected to invert the lidar signal by matching a segment of the lidar flight path to the MODIS AOD.

Figure 3 shows the summer 2003 comparison of Aqua satellite MODIS AOD at 550-nm with 5x5-km resolution to the lidar derived AOD from CAL for each flight date. High optical depths (> 0.3) are measured by MODIS throughout the San Joaquin Valley, as well as, near San Francisco and Los Angeles. Moving south from Stockton to Bakersfield, there appears to be an increase in aerosol loading. Table 2 provides a summary of each individual flight. The lidar ratios and Angstrom exponents are in the range of what is expected for urban/industrial aerosols or, in some cases, oceanic aerosols.

Figure 4 shows the 24-hr air mass back trajectories starting from Stockton, Fresno, and Bakersfield at 60-m and 2000-m altitudes calculated using the HYSPLIT model (available at http://www.arl.noaa.gov) along with particulate matter concentrations throughout the San Joaquin Valley at the time of the MODIS overpass. The majority of the trajectories indicate transport is contained within the valley or from the western part of California, with the exception of June 5 the June 17, which shows influence from eastern California/Nevada at an altitude of 2-km. Despite the high values of MODIS AOD, the PM2.5 concentrations are relatively low for the region. Using the values from the Stockton, CA ground monitor, $PM_{2.5}$ makes up 20%-25% of the PM10 mass concentration.

Figure 5 shows curtain plots of the lidar extinction measured at 1064-nm for each of the flight dates. The highest extinction values are measured near Bakersfield and the Tehachapi Mountains, as noted in the figures. The planetary boundary layer height for

the region is between 1.5 and 2-km. In the majority of the curtain plots, the peak in aerosol extinction is well above the surface, which may explain why the ground $PM_{2.5}$ mass concentrations do not measure the high level of aerosol loading that is measured by the MODIS instrument.

3.2 Winter 2007 Campaign

The Airborne HSRL AOD was obtained directly from the 532-nm wavelength lidar channel. Figure 6 shows the comparison between the lidar derived AOD and MODIS during the winter 2007 San Joaquin Valley campaign. Because both Aqua and Terra satellite overpasses occurred during the February 15 lidar flight, the lidar flight path is shown compared to both satellite MODIS AOD values. Similar to the summer 2003 campaign, the highest AOD are located in the central part of the Valley and near San Francisco and Los Angeles; however, the AOD values is lower than those measured during the 2003 summer. Table 3 provides a summary of each of the aircraft lidar flights. The standard deviations shown for the Angstrom exponent and 532-nm lidar ratio relate to the variability in the vertical profile of the two quantities. The Angstrom exponent and 532-nm lidar ratio are direct measurements from the HSRL lidar system, unlike the CAL data which require information from independent sources.

Figure 7 shows the 24-hr back trajectories from Stockton, Fresno, and Bakersfield at 60-m and 2000-m altitudes with $PM_{2.5}$ mass concentrations measured at the time of the lidar flight, during the 2007 campaign. Again, aerosol transport appears to be mostly contained within the valley, with air masses moving from north to south. One exception is on February 17, when surface-level winds originate from the east. Even though the measurements of optical depth are lower than those measured in 2003, the $PM_{2.5}$ mass

concentration in 2007 is nearly doubled compared to that of the summer campaign. Using the values obtained from the Fresno ground monitor, $PM_{2.5}$ makes up 56%-83% of the PM_{10} mass concentration.

Figure 8 shows the curtain plots of the 1064-nm aerosol extinction for each aircraft lidar flight. The planetary boundary layer is shallower than during the 2003 campaign, between approximately 1-km. The shallow boundary layer heights are believed to contribute to the increase in the ground $PM_{2.5}$ mass concentration. Aerosol particles that were trapped near the surface allowed more particulate matter to be measured than that in the case of elevated aerosols in the summer of 2003.

3.3 Bakersfield, CA Comparison

Bakersfield, CA, located in the southern end of the San Joaquin Valley, is the only city in flight range of both aircraft campaigns. Table 4 displays the lidar-derived AOD, PBL height, and $PM_{2.5}$ mass concentration measured during the closest aircraft lidar overpass for each campaign day and Table 5 shows the ratio of AOD to PBL height and the product of $PM_{2.5}$ mass concentration and PBL height. The ratio of total column AOD to the PBL height is nearly the same for both the winter and summer campaigns. Similarly, the product of the $PM_{2.5}$ mass concentration and PBL heights is nearly the same for both campaigns, which suggests an inverse relationship between the two.

Figure 9 shows the mean 1064-nm aerosol extinction profile near Bakersfield for the entire 2003 summer campaign compared with a similar profile from the 2007 winter campaign. As previously mentioned, the PBL height is much higher in the summer than in the winter. Also note the elevated peak in aerosol extinction during the summer campaign; whereas, aerosol extinction peaks near the surface during the winter.

3.4 Seasonal AOD-PM2.5 Comparisons

The 10x10-km operational MODIS AOD from Aqua was used to determine the mean AOD in the San Joaquin Valley for the months of February (winter) and June (summer) during the years between 2003 and 2008. Dates when cloud cover prevented AOD retrievals were removed from the comparison resulting in a total of 103 retrievals in winter and 174 retrievals in summer. Table 6 shows the comparison of the mean AOD within the San Joaquin Valley for each year. With the exception of 2007, the summer AOD is higher than the winter AOD. The largest percent differences between the summer and winter AOD occurred during years with large wildfires. Table 7 shows the comparison of $PM_{2.5}$ measured in Bakersfield (5558 California Avenue site) in the months of February and June for the years between 2003 and 2008. In all cases, PM2.5 concentration is highest in the summer.

The comparisons of AOD and PM2.5 generally agree with the findings of the 2003 and 2007 aircraft lidar campaigns. While the $PM_{2.5}$ mass concentration is always higher in the winter, the MODIS AOD is higher in the summer (with the exception of 2007). Over the six-year time period, the $PM_{2.5}$ in winter is 55% higher than the summer $PM_{2.5}$; however, the summer AOD is 43% higher than the winter AOD. A likely explanation is that in the summer elevated aerosols due to higher PBL heights and aloft layers due to wildfires add to the MODIS AOD, but do not contribute significantly to the $PM_{2.5}$ mass concentration measured at the surface.

4.0 Conclusions

Aircraft lidar campaigns in the summer (June 2003) and winter (February 2007) over the San Joaquin Valley are compared with AOD obtained from two different lidar

system, respectively, and MODIS sensors onboard Terra and Aqua satellites. MODIS AOD data is increasingly being used as an indication of ground air quality and in the San Joaquin Valley this is important as the Valley has significant air quality concerns. While satellite data gives a broad area picture of the AOD, it does not give the vertical distribution of the AOD which is why lidar measurements are needed to determine the AOD and aerosol vertical distribution. This data must then be correlated with ground based $PM_{2.5}$ measurements to understand the air quality throughout the Valley.

Lidar measured AOD compared well with MODIS AOD when there was overlap with MODIS pixels and the lidar flights. AOD tended to be higher in the summer than in the winter campaign and highly non-uniform throughout the Valley. Generally AOD increased toward the lower Valley. The two lidar campaigns had different flight tracks, but they did overlap in the Bakersfield, CA area where the summer lidar had an average AOD of 0.21 with a ground $PM_{2.5}$ of 16.6 micrograms per cubic meter and the winter lidar had an average AOD of 0.15 with a ground $PM_{2.5}$ of 29.3 micrograms per cubic meter. The corresponding average planetary boundary layer height (PBL) was 1.54 and 1.0 km. This suggested that in the winter the reduced PBL increased the $PM_{2.5}$ measured on the ground. While the $PM_{2.5}$ sources are different in the summer and winter seasons, the PBL does seem to play a significant role in the $PM_{2.5}$ as measured on the ground. If the PBL height and the associated $PM_{2.5}$ are multiplied together the summer value is 25.6 and the winter value is 29.2 (micrograms per cubic meter km) nearly the same for the Bakersfield area. It would be interesting to determine if this value remains constant throughout the year resulting in a straightforward way to determine $PM_{2.5}$ by measuring local AOD. The summer lidar profiles consistently showed an increase in extinction

above the ground making the use of MODIS AOD as an indicator of ground $PM_{2.5}$ problematic.

The increased use of ground based aerosol lidars in the Valley could, along with the broader area MODIS AOD data, substantially improve the understanding of air quality within the Valley.

Acknowledgements
The authors would like to thank James J. Szykman, Jassim A. Al-Saadi, Chris A. Hostetler, Johnathan W. Hair, Anthony L. Cook, David B. Harper, and Richard A. Ferrare for the collection and use of the 2007 San Joaquin Valley HSRL data.

REFERENCES

Al-Saadi, J.A. and Coauthors (2008): Application of satellite aerosol optical depth and airborne lidar data for monitoring fine particulate formation and transport in San Joaquin Valley, California. Preprints, *10th Conference on Atmospheric* Chemistry, New Orleans, LA, Amer. Meteor. Soc.

De Young, R.J., W.B. Grant, and K. Severance (2005): Aerosol Transport in the California Central Valley Observed by Airborne Lidar. *Environ. Sci. Technol.*, **39**, 8351-8357.

Fernald, F.G., 1984: Analysis of atmospheric lidar observations: Some comments. *Appl. Opt.*, **23**, 652–653.

Fernald, F.G., B.M. Herman, and A. Reagan, 1972: Determination of aerosol height distributions by lidar. *Appl. Meteorol.*, **11**, 482-489.

Geis, Sonya (2007, October 8): Smog traps California community. *Washington Post*, p. A03.

Gili, C. and R. De Young (2006): A compact efficient lidar receiver for measuring atmospheric aerosols. NASA Tech. Rep., NASA/TP-2006-213950, 19 pp.

Hair, J.W. and Coauthors (2008): Airborne high spectral resolution lidar for profiling aerosol optical properties. *Appl. Opt.*, **47**, 6734-6753.

Kumar, N., A. Chu, and A. Foster, 2007: An empirical relationship between PM2.5 and aerosol optical depth in Delhi Metropolitan. *Atmos. Environ.*, **41**, 4492–4503.

Kumar, N., A. Chu, and Andrew Foster, Remote Sensing of Ambient Particles in Delhi and its Environs: Estimation and Validation, *Int. J. Remote Sens*., 29(12), 3383-3405, 2008

Remer, L.A. and Coauthors, 2006, Algorithm for remote sensing of tropospheric aerosol from land: collection 5, http://modis-atmos.gsfc.nasa.gov/references, ATBD-MOD-96, NASA Goddard Space Flight Center.

San Joaquin Valley Air Pollution Control District (2008a): Annual report to the community. Retrieved March 9, 2009 from http://www.valleyair.org/General_info/pubdocs/2008AnnualReportfinal-web.pdf

San Joaquin Valley Air Pollution Control District (2008b): 2008 PM2.5 Plan – Final Adopted April 30, 2008. Retrieved March 9, 2009 from http://www.valleyair.org/air_quality_plans/AQ_Final_Adopted_PM25_2008.htm

Sasano, Y. and E.V. Browell (1989): Light scattering characteristics of various aerosol types derived from multiple wavelength lidar observations. *Appl. Optics*, **28** (9), 1670-1679.

Smith, T.B, D.E. Lehrman, D.D. Reible, and F.H. Shair (1981): A Study of the Origin and Fate of Air Pollutants in California's Sacramento Valley, Final Report to the California Air Resources Board, December 1981.

Strawbridge, K.B. and R.M. Hoff (1996): LITE validation experiments along California's coast: preliminary results. *Geo. Res. Lett.*, **23**, 73-76.

TABLE 1. Summary of lidar properties for CAL and Airborne HSRL lidars

		CAL	HSRL
Laser			
	Manufacturer	Big Sky (Quantel)	Fibertek
	Repetition rate	20-Hz	200-Hz
	Beam divergence	1.5-mrad	0.8-mrad
	1064-nm energy	60-mJ	1.1-mJ
	532-nm energy	80-mJ	2.5-mJ
Telescope			
	Diameter	0.30-m	0.40-m
	FOV	1.6-mrad	1.0-mrad
Filters			
	1064-nm	1-nm, FWHM	0.4-nm, FWHM
	532-nm	0.5-nm, FWHM	60-pm (etalon), FWHM
Detectors			
	1064-nm channel	APD (analog)	APD (analog)
	532-nm channel	PMT (analog & photon counting)	PMT (analog)

TABLE 2. Summary of summer 2003 San Joaquin Valley campaign.

Date	Takeoff (UTC/PST)	MODIS Overpass (UTC)	Altitude (km)	Angstrom exponent	1064-lidar ratio (sr)
June 3, 2003	23:40/16:40	Aqua 21:05	6	1.451	45
June 5, 2003	22:39/15:39	Aqua 20:55	11	1.436	30
June 5, 2003	27:16/20:16	Aqua 20:55	12	1.436	16
June 11, 2003	27:16/20:16	Aqua 20:15, 20:20	12	1.060	20
June 12, 2003	23:33/16:33	Aqua 21:00	12	1.151	12-20
June 17, 2003	19:55/12:55	Aqua 21:20	6	1.377	35

TABLE 3. Summary of winter 2007 San Joaquin Valley campaign.

Date	Takeoff (UTC/PDT)	MODIS Overpass (UTC)	Altitude (km)	Angstrom exponent	532-lidar ratio (sr)
Feb. 15, 2007	19:58/11:58	Terra 19:25 Aqua 21:05	8.8	1.40 ± 0.09	45.3 ± 5.7
Feb. 16, 2007	15:58/7:58	Terra 18:30	8.9	1.31 ± 0.06	59.0 ± 8.9
Feb. 16, 2007	20:49/12:49	Aqua 21:45	8.9	1.46 ± 0.13	40.3 ± 10.0
Feb. 17, 2007	18:10/10:10	Terra 19:15	8.8	1.44 ± 0.09	51.2 ± 4.2
Feb. 17, 2007	23:53/15:53	Aqua 20:50	8.8	1.44 ± 0.13	46.6 ± 5.8

TABLE 4. Comparison of Bakersfield, CA lidar and $PM_{2.5}$ data

2003 summer campaign				2007 winter campaign			
Date	AOD	PBL height (km)	$PM_{2.5}$ ($\mu g\ m^{-3}$)	Date	AOD	PBL height (km)	$PM_{2.5}$ ($\mu g\ m^{-3}$)
June 3	0.2472	1.63	19.5	Feb. 15	0.1855	1.32	18.9
June 5	0.2423	1.57	21.9	Feb. 16	0.2020	1.11	35.8
June 5	0.2579	1.81	17.0	Feb. 16	0.2371	1.17	29.7
June 11	0.2244	1.24	9.0	Feb. 17	0.0604	0.51	32.1
June 12	0.1696	1.54	18.5	Feb. 17	0.0504	0.87	30.0
June 17	0.1145	1.47	13.5				
Mean	**0.2093**	**1.54**	**16.6**	**Mean**	**0.1471**	**1.00**	**29.3**
St. Dev.	**0.056**	**0.19**	**4.6**	**St. Dev.**	**0.086**	**0.32**	**6.3**

Table 5. Relationship between AOD, PBL, and $PM_{2.5}$ in Bakersfield, CA

	2003 summer campaign	2007 winter campaign
AOD PBL^{-1} ± SD (km^{-1})	0.136 ± 0.037	0.140 ± 0.057
$PM_{2.5}$ × PBL ± SD ($\mu g\ m^{-3}$ km)	25.6 ± 9.1	29.2 ± 9.1

Table 6. Yearly comparison of AOD within the San Joaquin Valley (SJV)

	Mean AOD within SJV		% Difference
Year	Winter (February)	Summer (June)	
2003	0.0758	0.1620	72
2004	0.0911	0.1146	23
2005	0.1237	0.1438	15
2006	0.1035	0.2130	69
2007	0.1412	0.1154	-20
2008	0.1293	0.3087	82
6-year	**0.1150**	**0.1783**	**43**

Table 7. Yearly comparison of $PM_{2.5}$ mass concentration in Bakersfield, CA

	Mean PM2.5 from Bakersfield-5558 CA ($\mu g/m^3$)		% Difference
Year	Winter (February)	Summer (June)	
2003	25	17	38
2004	16	13	21
2005	30	13	79
2006	30	14	73
2007	32	13	84
2008	33	26	24
6-year	**28**	**16**	**55**

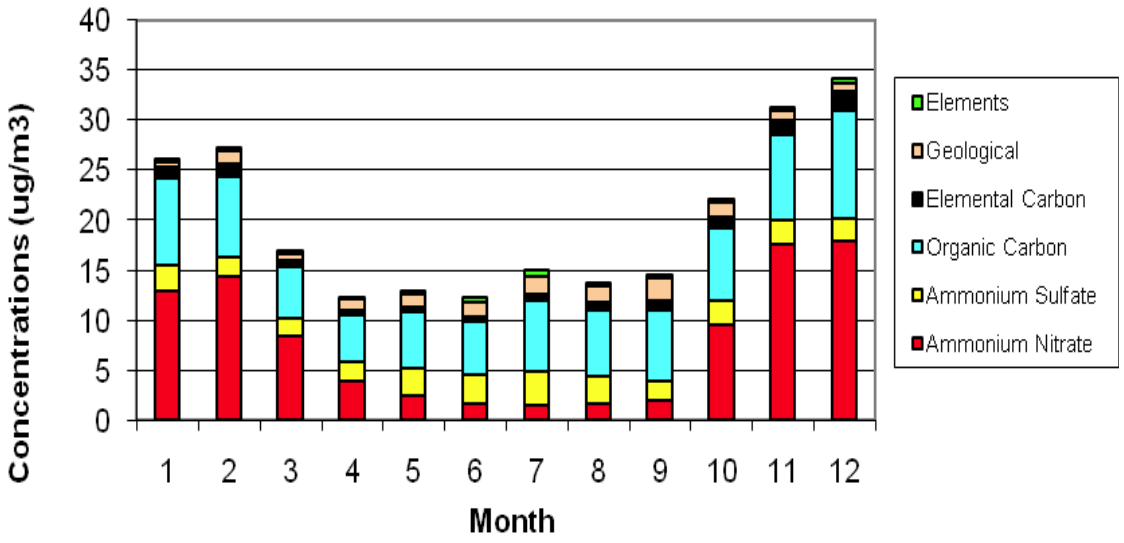

Fig. 1. Seasonal pattern and composition of $PM_{2.5}$ near Bakersfield, CA from San Joaquin Valley Air Pollution Control District, 2008 $PM_{2.5}$ Plan - Final Adopted.

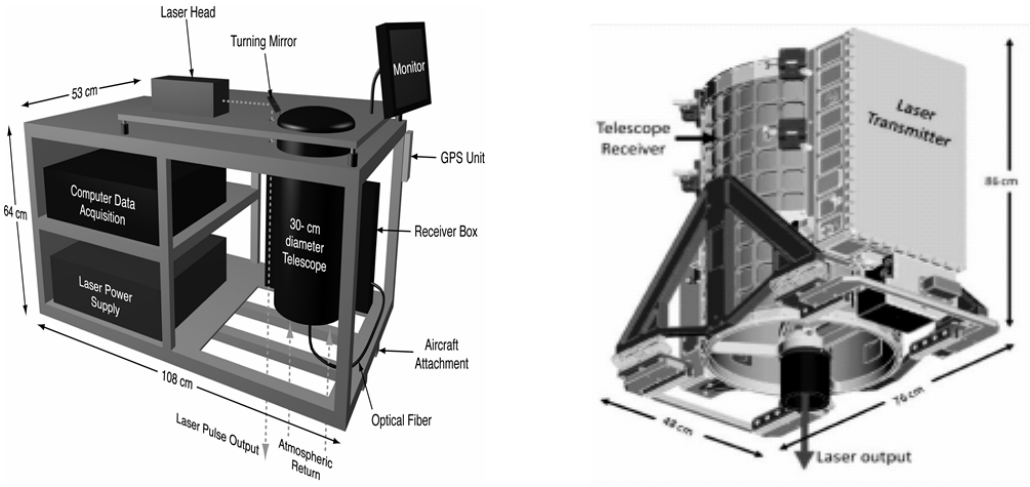

Figure 2. Left, compact aerosol lidar (CAL) system for aircraft deployment; and Right, airborne high spectral resolution lidar (HSRL) configured for aircraft deployment.

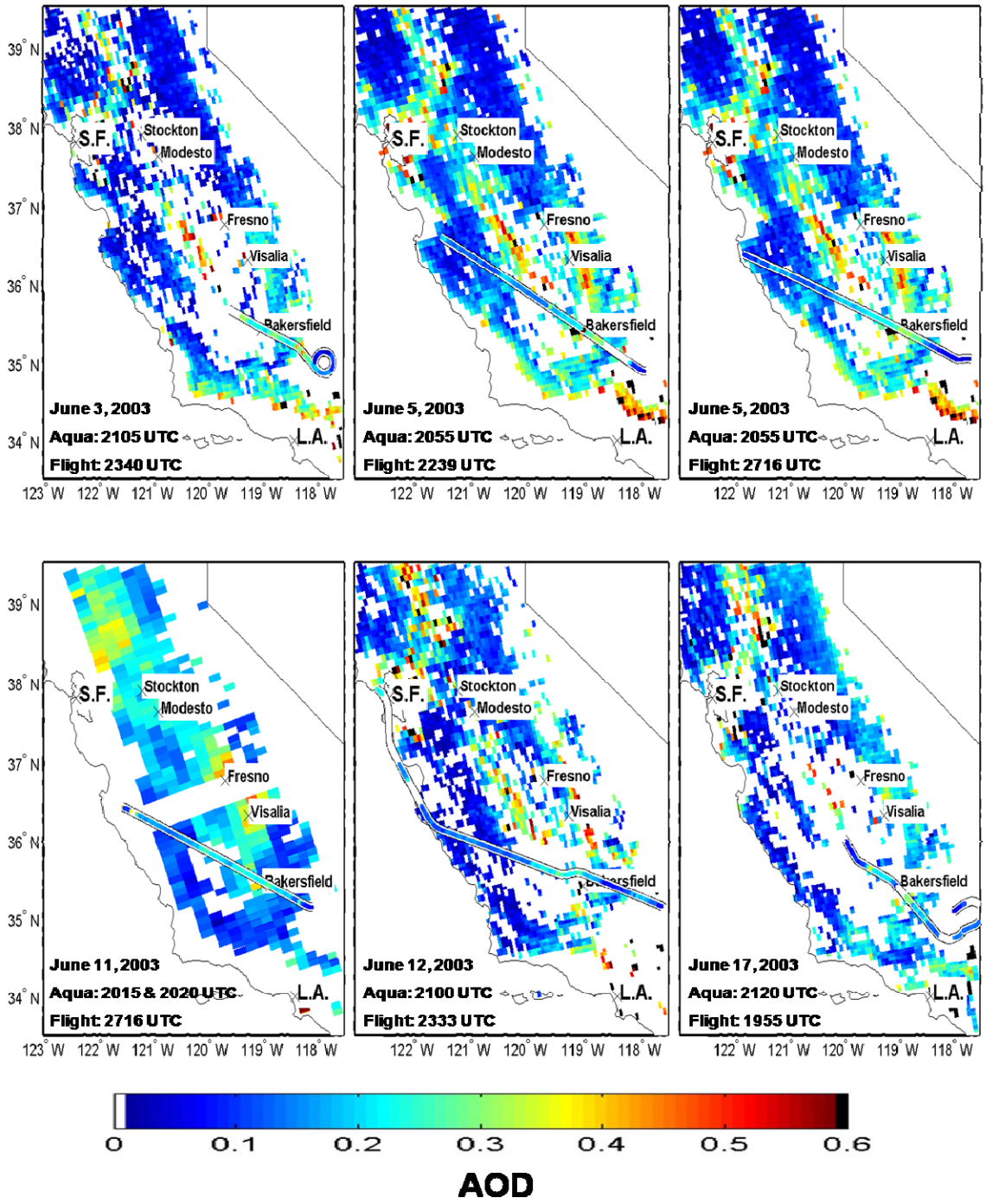

Figure 3. Summer 2003 comparison of MODIS (550-nm) 5x5-km AOD and flight tracks for CAL (converted 532-nm) AOD in the San Joaquin Valley, California.

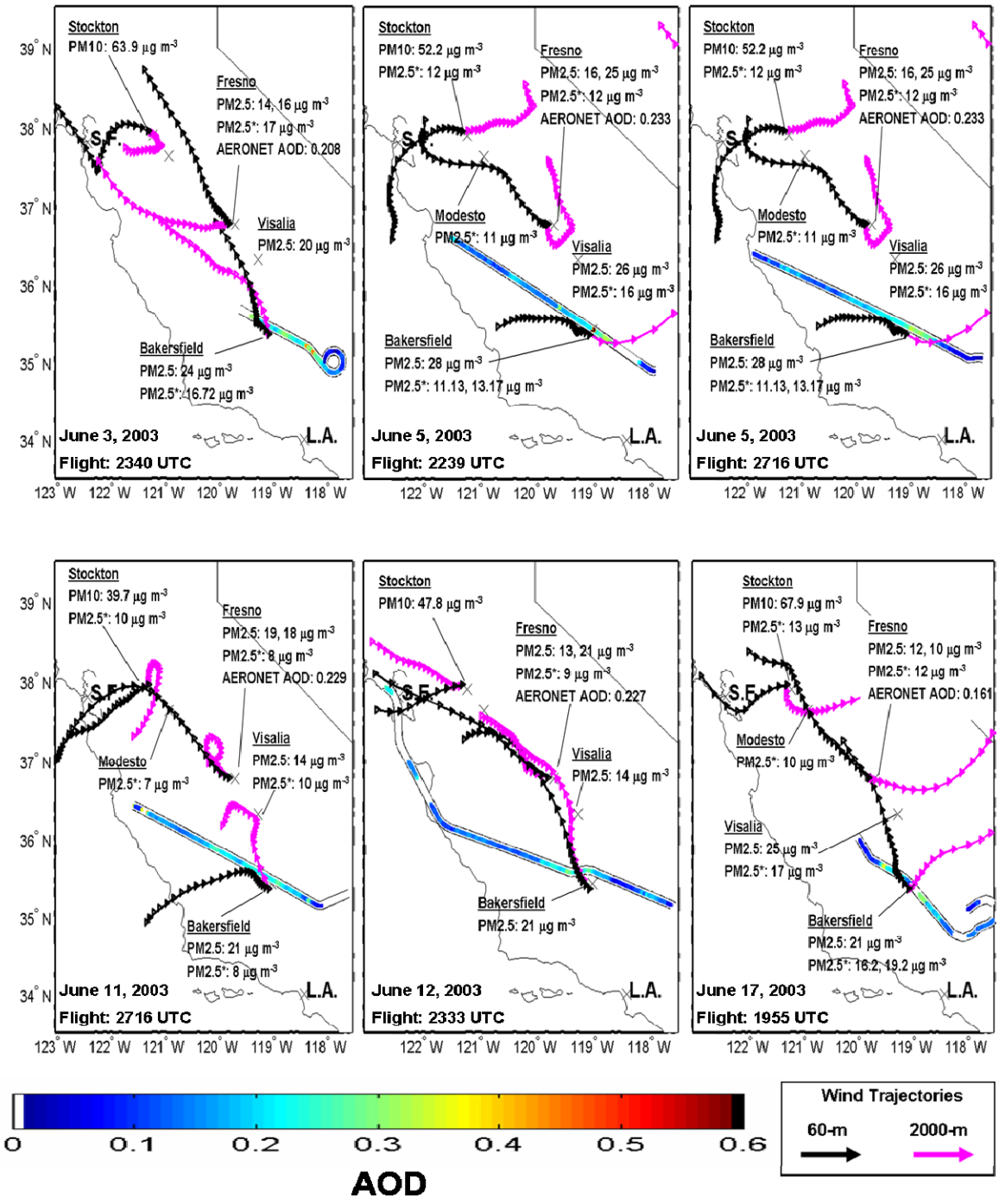

Figure 4. AOD of CAL flight track with back trajectories (markers represent 1-hour time intervals) at different altitudes (shown in different colors), PM_{10} and $PM_{2.5}$ mass concentrations at the time of the nearest MODIS overpass, and AERONET AOD measured at Fresno, CA during the summer 2003 San Joaquin Valley campaign. The PM2.5* denotes 24-hr averages.

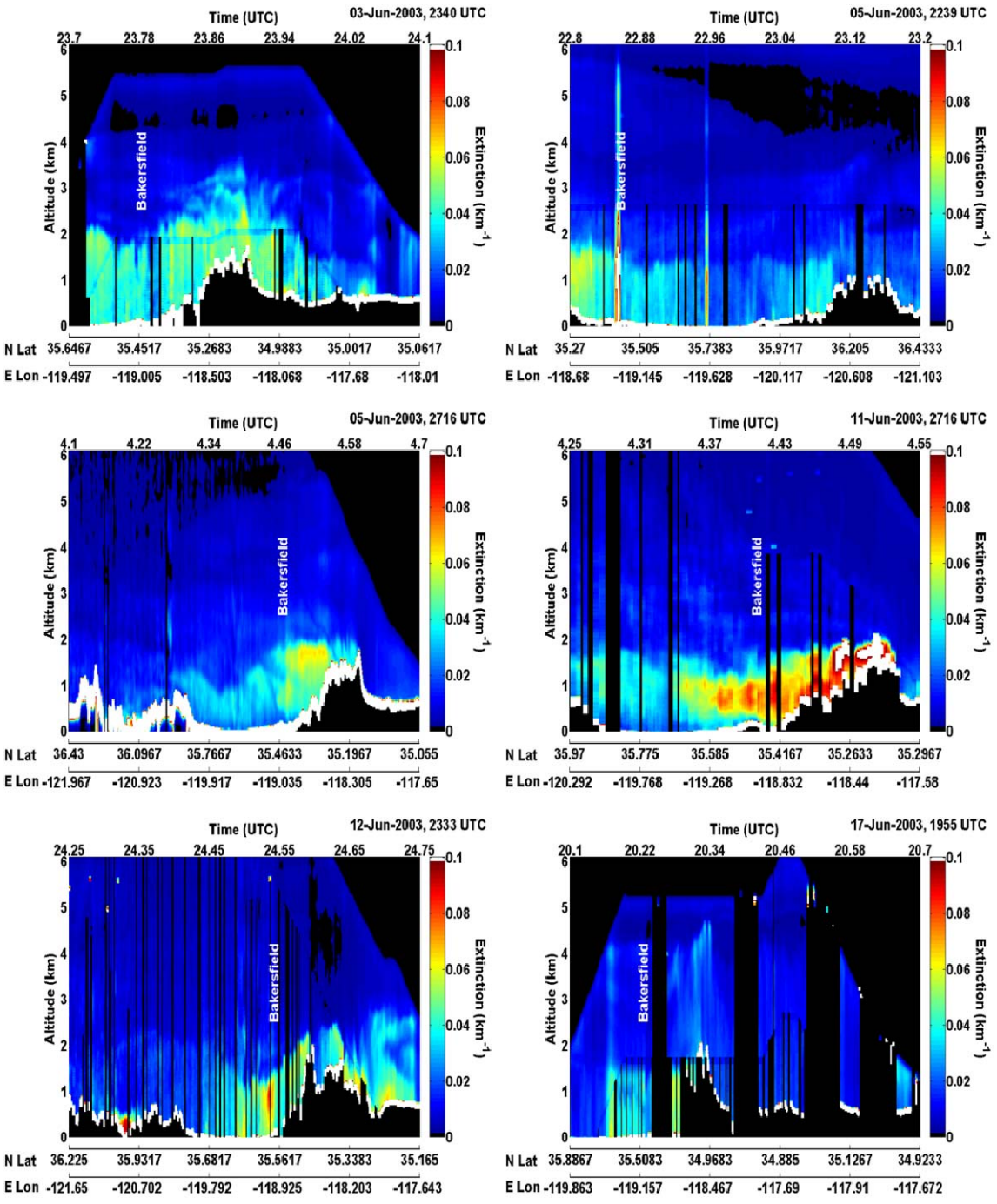

Figure 5. Curtain plots of the 1064-nm lidar extinction during the summer 2003 San Joaquin Valley campaign. Bakersfield, CA is indicated in each plot.

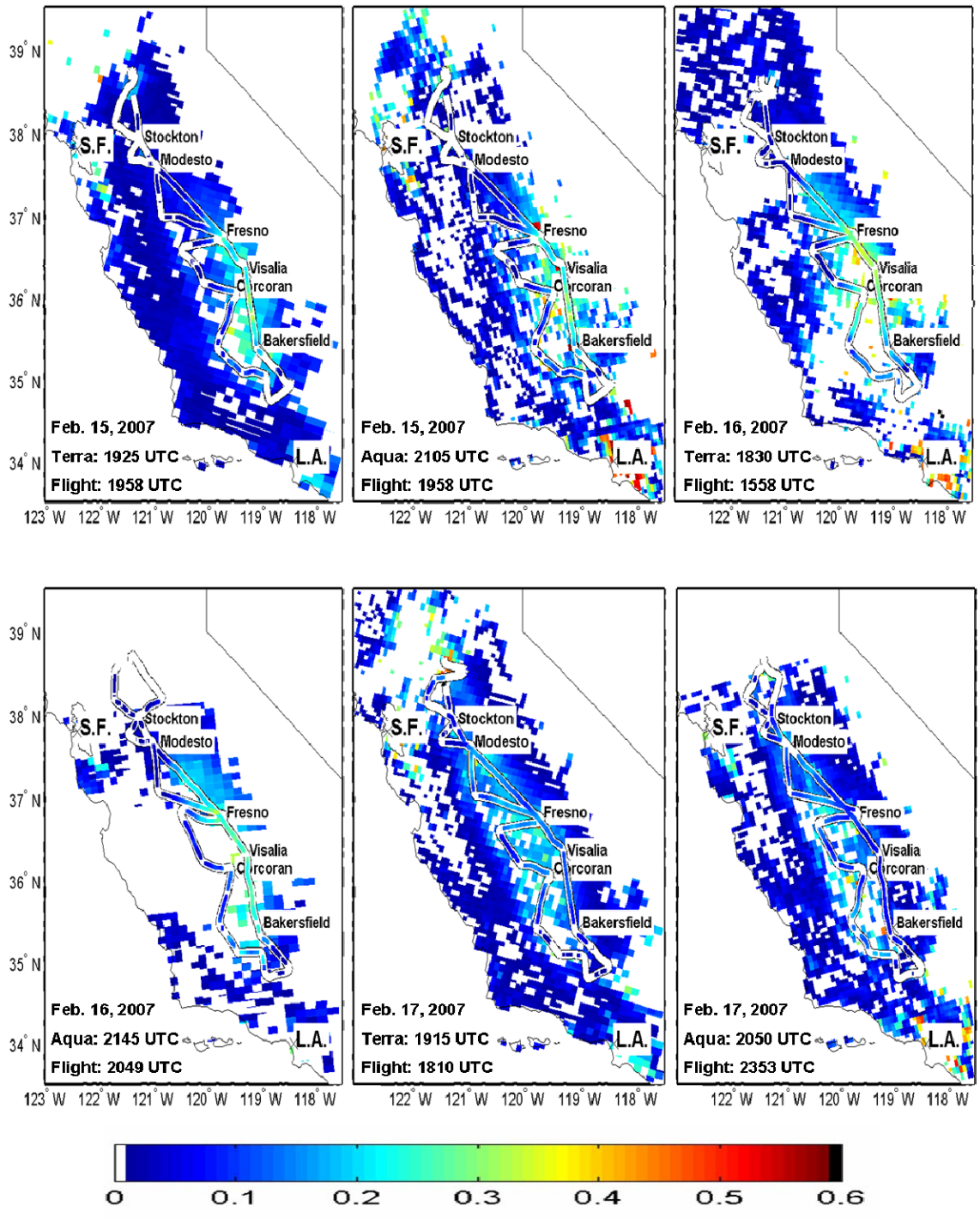

Figure 6. Winter 2007 comparison of MODIS (550-nm) 5x5-km AOD and flight tracks for HSRL (532-nm) AOD in the San Joaquin Valley, California.

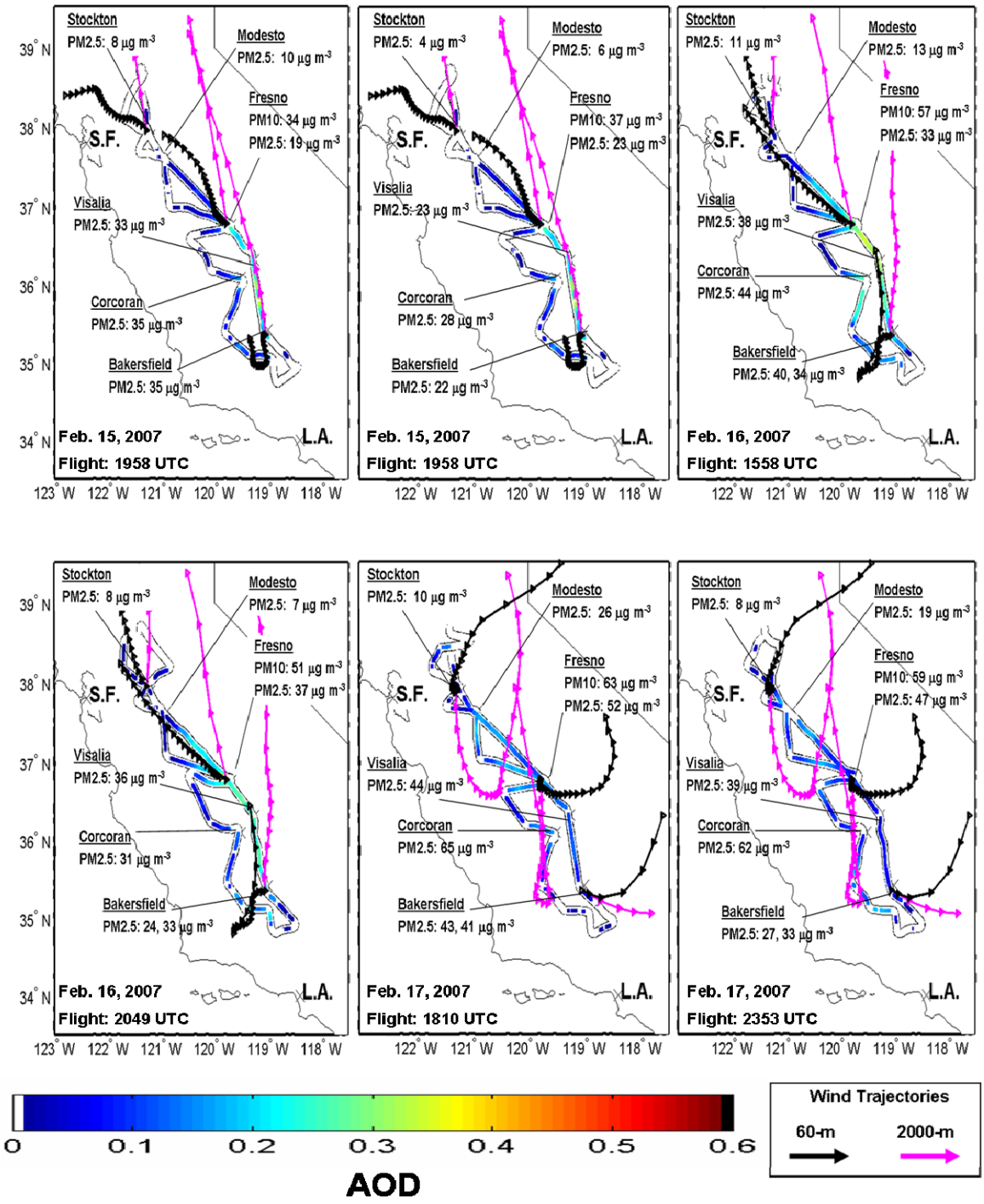

Figure 7. AOD of HSRL flight track with back trajectories (markers represent 1-hour time intervals) at different altitudes (shown in different colors), PM_{10} and $PM_{2.5}$ mass concentrations at the time of the nearest MODIS overpass during the winter 2007 San Joaquin Valley campaign.

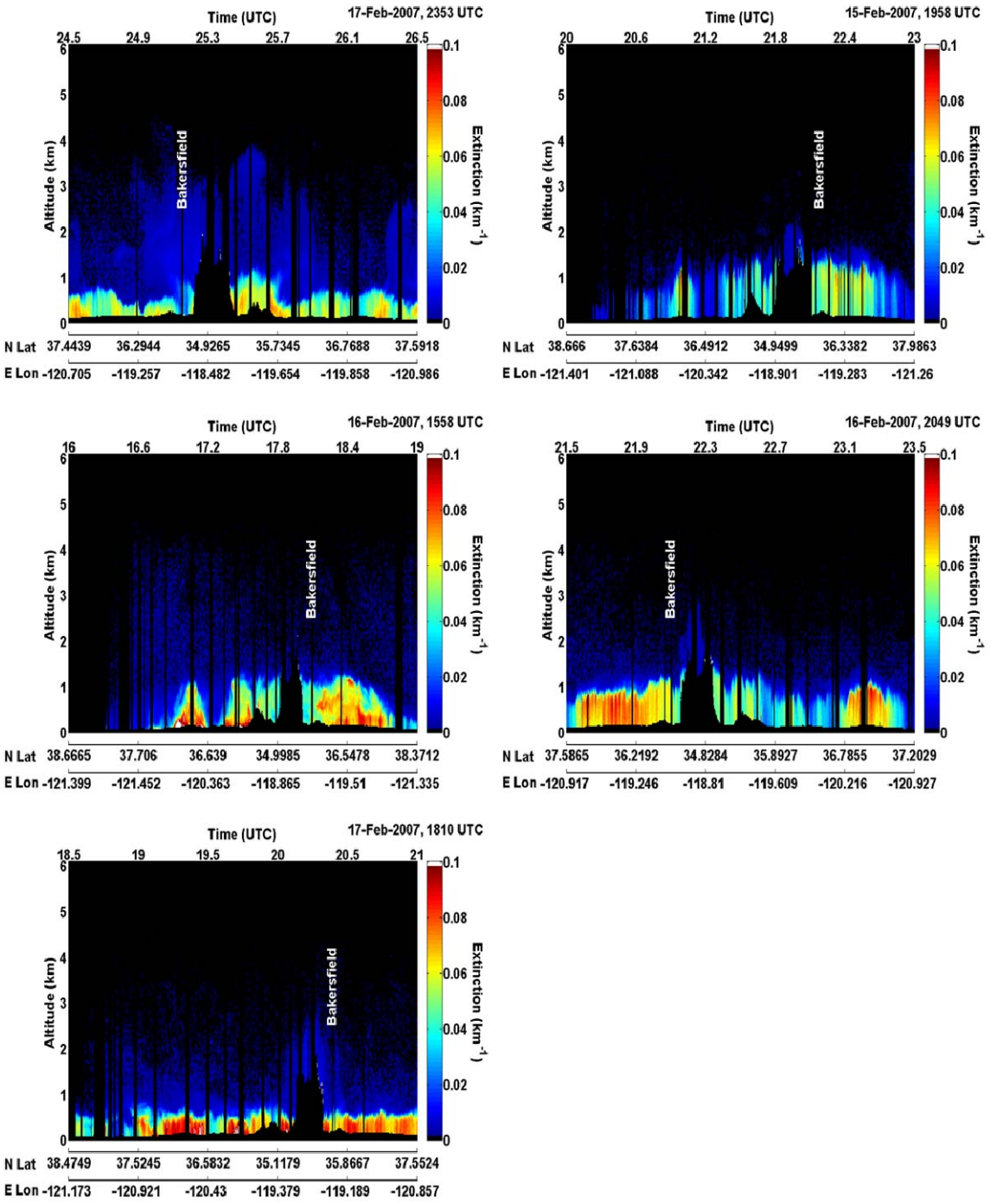

Figure 8. Curtain plots of the 1064-nm lidar extinction during the winter 2007 San Joaquin Valley campaign. Bakersfield, CA is indicated in each plot.

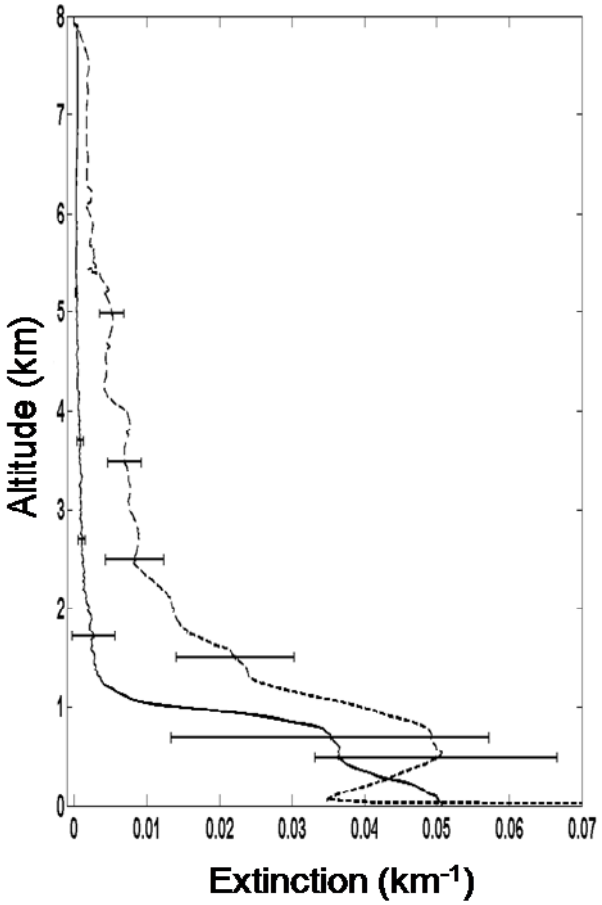

Figure 9. Comparison of mean 1064-nm aerosol extinction profiles near Bakersfield, CA for summer 2003 campaign (dashed line) and 2007 winter campaign (solid line).